Editors' Suggestion | Featured in Physics

Demonstration of a Timescale Based on a Stable Optical Carrier

William R. Milner,[1,*] John M. Robinson,[1] Colin J. Kennedy,[1] Tobias Bothwell,[1] Dhruv Kedar,[1] Dan G. Matei,[2] Thomas Legero,[2] Uwe Sterr,[2] Fritz Riehle,[2] Holly Leopardi,[3] Tara M. Fortier,[3] Jeffrey A. Sherman,[3] Judah Levine,[3] Jian Yao,[3,†] Jun Ye,[1,‡] and Eric Oelker[1,§]

[1]*JILA, NIST and University of Colorado, 440 UCB, Boulder, Colorado 80309, USA*
[2]*Physikalisch-Technische Bundesanstalt, Bundesallee 100, 38116 Braunschweig, Germany*
[3]*National Institute of Standards and Technology, 325 Broadway, Boulder, Colorado 80305, USA*

(Received 6 July 2019; published 21 October 2019)

We report on the first timescale based entirely on optical technology. Existing timescales, including those incorporating optical frequency standards, rely exclusively on microwave local oscillators owing to the lack of an optical oscillator with the required frequency predictability and stability for reliable steering. We combine a cryogenic silicon cavity exhibiting improved long-term stability and an accurate ^{87}Sr lattice clock to form a timescale that outperforms them all. Our timescale accumulates an estimated time error of only 48 ± 94 ps over 34 days of operation. Our analysis indicates that this timescale is capable of reaching a stability below 1×10^{-17} after a few months of averaging, making timekeeping at the 10^{-18} level a realistic prospect.

DOI: 10.1103/PhysRevLett.123.173201

Accurate and precise timing is critical for a wide array of applications, ranging from navigation and geodesy to studies of fundamental physics [1–6]. The worldwide time standard, Coordinated Universal Time (UTC), is synthesized from a global network of atomic clocks and disseminated at monthly intervals. National metrology institutes bridge the gap between updates of UTC by broadcasting independent timescales derived from ensembles of microwave local oscillators steered to accurate atomic frequency standards [7,8]. To advance the frontier of precision timekeeping, the development of both improved local oscillators and atomic frequency standards is imperative.

Optical atomic clocks, currently up to 2 orders of magnitude more accurate and stable than their microwave counterparts [4,9–13], show promise as frequency standards for timescale applications. Recent efforts to incorporate optical clocks into existing microwave timescales have led to improved performance [14–16]. However, despite the fact that optical clocks have demonstrated mid-10^{-17} level stability in 1 s of averaging [17,18], timescales steered to optical standards have thus far required weeks of averaging to reach 10^{-16} level precision [16,19]. This disparity in performance arises due to down-conversion of noise from the local oscillator—a consequence of steering to an atomic standard in the presence of dead time—which degrades the long-term stability of the timescale [16]. This limitation is motivation for the development of local oscillators with improved stability, particularly at averaging times around the typical interval between clock measurements (10^3–10^5 s). In parallel, improvements in local oscillator stability allow a timescale to maintain a competitive level of performance even when relaxing the requirements on optical clock uptime.

In this Letter, we report on the first realization of a timescale based on an optical local oscillator (OLO) which outperforms state-of-the-art microwave oscillators steered to either microwave or optical frequency standards. This all-optical timescale consists of an ultrastable laser based on a cryogenic silicon reference cavity that is steered daily to an accurate ^{87}Sr lattice clock [20] over a monthlong campaign. During this period, the frequency stability of the OLO surpasses that of the hydrogen masers in the UTC (NIST) timescale at all averaging intervals up to multiple days [21], demonstrating the requisite stability for improved timescale performance. Our analysis indicates that daily steering of the OLO frequency with 50% clock uptime allows for a timescale instability below the 10^{-17} level within 85 days of operation. Our local oscillator frequency is easily predictable using conventional timescale steering algorithms, allowing us to limit the estimated time error to only 48 ± 94 ps after 34 days of operation. The continuous availability of the OLO coupled with the on-demand performance of our optical clock make our system viable for future inclusion in UTC (NIST). This new variant of timescale harnesses both the improved accuracy and stability of optical standards and provides a viable blueprint for the upgrade of timescales worldwide.

After a decade of development [22,23], cryogenic silicon reference cavities are now a proven platform for laser stabilization at the mid-10^{-17} level [24,25]. The exceptional short-term stability of these local oscillators has enabled advances in optical clock stability [17]. These systems outperform all free-running local oscillators at averaging times below 1×10^4 s [17] and exhibit orders-of-magnitude lower frequency drift than other OLOs [24,26]. However,

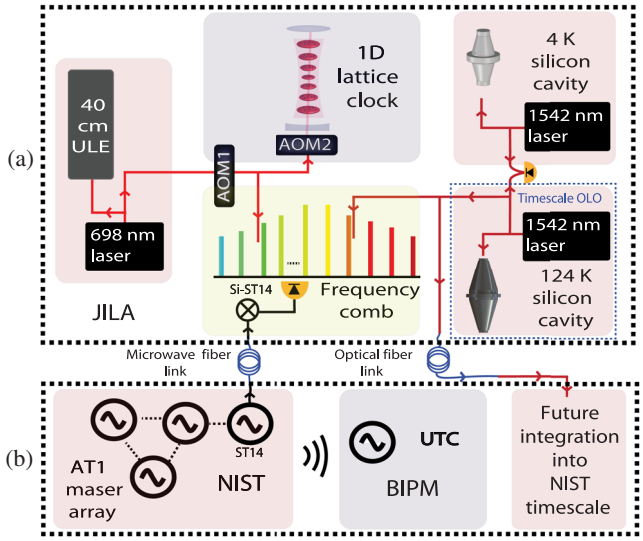

FIG. 1. (a) An array of three lasers are locked to ultrastable Fabry-Perot resonators. A femtosecond frequency comb transfers the stability of the OLO (124 K Si cavity) from 1542 nm to a prestabilized laser at 698 nm used to perform clock spectroscopy in a one-dimensional (1D) ^{87}Sr lattice clock. (b) AT1, a free running microwave timescale at NIST, is compared continuously against the OLO signal over a fiber-optic link using a hydrogen maser (ST14) as a transfer oscillator. An optical fiber link between JILA and NIST allows for stable transfer of the optical timescale to NIST for future integration into UTC (NIST) and for broadcast to the International Bureau of Weights and Measures (BIPM).

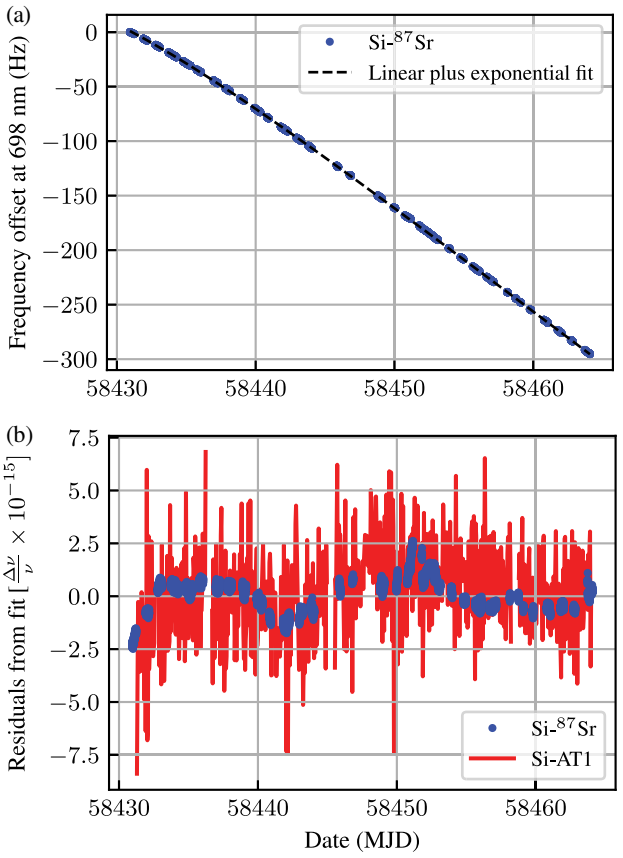

FIG. 2. (a) The OLO frequency (Si) is measured at 698 nm using a ^{87}Sr lattice clock. A linear plus exponential trend, $a + bt + ce^{-(t/d)}$, agrees well with the raw frequency data. The fit parameters are $a = 24.16$ Hz, $b = -9.632$ Hz/day, $c = -23.17$ Hz, and $d = 7.813$ days. (b) The residuals of the OLO comparisons against the ^{87}Sr clock and the NIST AT1 timescale after subtracting the drift trend from (a) from both datasets.

achieving a stability commensurate with the best microwave oscillators at longer averaging times has remained an elusive goal, hampering their usefulness as timescale flywheel oscillators. The OLO used in our timescale, based on a 21 cm long Si cavity operating at 124 K, was recently optimized to significantly improve its long-term stability. The use of superpolished optics and thermal control of the environment limit parasitic etalons, and active optical power stabilization reduces frequency excursions from laser intensity drift [21,27–29].

We combine our local oscillator with an accurate optical frequency standard to form an all-optical timescale. Over a 34 day interval, a strontium lattice clock with systematic uncertainty of 2.0×10^{-18} [20] is used to track the OLO frequency with 25% uptime. Daily measurements of the OLO allow us to build a reliable predictive model of its frequency evolution. As new frequency data become available, the model is updated to better reflect its current behavior. The OLO is steered using the model to correct for changes in its frequency over time, and any residual frequency fluctuations ultimately determine the timescale stability. The analysis required to realize the timescale was carried out in postprocessing, though we emphasize that our approach is compatible with real-time implementation.

To track frequency excursions larger than the low-10^{-16} level during intervals when the optical clock is off-line, the OLO must be compared with two independent ultrastable lasers based on a 6 cm silicon cavity operated at 4 K [24] and a 40 cm ultralow expansion (ULE) cavity [30]. Because the three systems have comparable short-term stability, one may use a three-cornered hat analysis to identify any significant frequency jumps in the OLO and update the predictive model accordingly [21].

A schematic of our optical timescale is presented in Fig. 1(a). In order to reference the ^{87}Sr clock laser to the 124 K silicon cavity, we transfer its optical stability from 1542 nm to a prestabilized laser at 698 nm using a femtosecond Er:fiber frequency comb with negligible additive instability [17]. The frequency corrections applied to AOM1 by the stability transfer servo are recorded to monitor the relative frequency fluctuations between the 40 cm ULE cavity and the OLO. The stabilized 698 nm light is then tuned to resonance for the ^{87}Sr clock transition using AOM2. The AOM2 correction signal is recorded and yields the OLO frequency relative to the ^{87}Sr transition. An optical beat note at 1542 nm between the OLO and the 6 cm

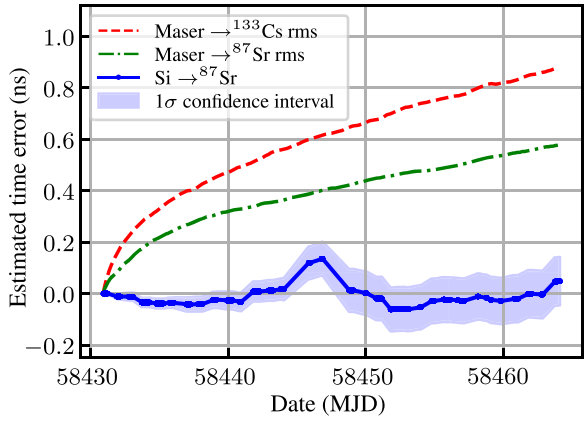

FIG. 3. An estimate of the time error evolution of the optical timescale over the 34 day data campaign results in an integrated value of 48 ± 94 ps. The peak-to-peak value of 197 ps is dominated by a 4 day window that includes the two days when the ^{87}Sr clock was not operated. The rms spread in time error for two timescales based on repeated simulations of a maser steered to either a microwave or optical frequency standard are shown for comparison [21].

Si cavity serves as a continuous monitor of their frequency difference. Figure 1(b) depicts AT1, a free-running microwave timescale at NIST. Using a hydrogen maser as a transfer oscillator, AT1 is compared remotely with the local oscillator over a stabilized fiber-optic link [21,31]. To enable this comparison, the OLO is down-converted to the rf domain using a frequency comb. This provides an additional record of the long-term performance of the OLO that is nearly continuous (95% uptime) over the measurement campaign. We note that AT1 is chosen rather than UTC (NIST) due to its superior stability over the averaging intervals of relevance to this study.

A record of the OLO frequency during the data campaign spanning from a modified Julian date (MJD) of 58 430 to 58 464 is presented in Fig. 2(a). The clock ran daily with the exception of MJD 58 444 and 58 447. Three days before the first measurement, the optical power incident on the cavity was changed to reset an intensity noise servo. Consistent with prior silicon cavity drift studies, the frequency evolution of the OLO after adjusting the incident optical power is well modeled by a constant linear drift plus an exponential relaxation term: $a + bt + ce^{-(t/d)}$ [24]. Figure 2(b) shows the residuals of the OLO comparisons with the clock and AT1 after subtracting the modeled drift trend determined by a fit to the ^{87}Sr clock data. Perfect correlation between the two datasets is not expected, as both AT1 and the microwave link contribute additional instability to the Si-AT1 record [21].

During the interval between clock operation on MJD 58 441 and 58 442, two frequency jumps on the OLO were identified with a combined amplitude of 5.02×10^{-15}. A correction of the same magnitude is applied to all data after this step when performing the analysis presented in this Letter. No significant change in the long-term drift trend of the local oscillator was observed following these excursions. Under real-time operating conditions, we anticipate an additional time error of less than 5 ps from these two jumps [21].

To realize a timescale, the OLO frequency record in Fig. 2(a) is steered using a predictive model to minimize its offset from the atomic frequency standard. The predictive model utilizes a Kalman filter to estimate the frequency of the OLO at a given time based on prior measurements with the clock. Kalman filtering techniques are commonly used in time scales to model the frequency of hydrogen masers [32,33]. The drift in the OLO frequency between daily measurements is well approximated by a quadratic function: $k_0 + k_1 t + (k_2 t^2/2)$. The model prediction is determined by a state vector $[k_0, k_1, k_2]$ that is updated epoch by epoch when the ^{87}Sr clock is running. We stress that this technique does not utilize *a priori* knowledge of the drift coefficients from Fig. 2(a). When the clock is on-line, the Kalman filter adapts rapidly to follow the current drift trend of the cavity and the prediction remains accurate provided that the drift does not change significantly between daily measurements. Further detail on the Kalman filter algorithm is provided in Refs. [21,34].

To evaluate the performance of a timescale, one typically compares it against a reference timescale with significantly lower timing uncertainty. To our knowledge, no such timescale exists in this case. Instead, we treat the ^{87}Sr clock as an ideal frequency reference and examine the fractional frequency offset between the steered OLO record and the clock transition frequency, hereafter referred to as the prediction error. We define the time error of our timescale as the integral of the prediction error over time.

If the frequency record were continuous, the time error could be determined to within the measurement precision of the clock. However, a finite gap of time separates the frequency measurements in Fig. 2(a), ranging from the 5 s interrogation cycle of our experiment to 24 h between daily measurements. Most of the time error accumulates during the longer gaps, when the Kalman filter must accurately predict changes in the OLO frequency without new measurement data from the clock. The time error contribution from a gap is simply the gap duration multiplied by the mean prediction error during this interval. However, the latter quantity cannot be determined exactly from the available data. Instead, we estimate the mean prediction error by averaging the values before and after the gap and multiply by the gap duration to compute an estimated time error. We compute a 1σ confidence interval for the estimated time error through repeated simulations of the OLO frequency during each gap [21].

An estimate of the integrated time error of our optical timescale is presented in Fig. 3. After 34 days of integration, our timescale accumulates an error of 48 ± 94 ps. For comparison, we simulate timescales consisting of a hydrogen maser steered to a ^{133}Cs fountain for 24 h/day and a

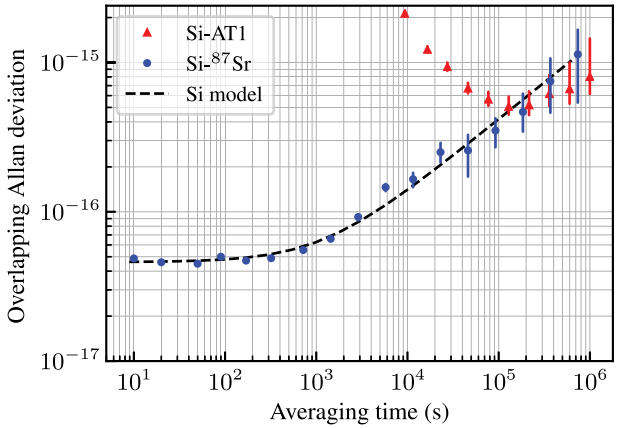

FIG. 4. The silicon cavity stability is computed from the detrended ^{87}Sr data in Fig. 2(b) using a gap-tolerant Allan variance similar to Ref. [36]. The data are fit to a noise model with an instability of $\sigma = 1.3 \times 10^{-18}\sqrt{\tau(\mathrm{s})}$ at long averaging times. The long-term stability of the OLO is also inferred from a continuous measurement against the NIST AT1 timescale.

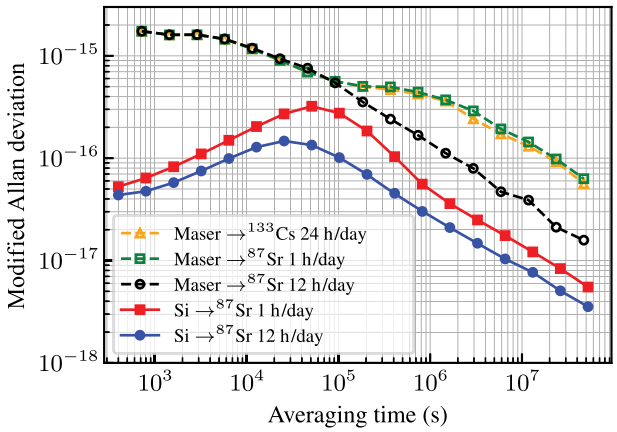

FIG. 5. Expected fractional frequency stability of the optical timescale. The stability of our optical timescale is analyzed for two optical clock duty cycles. Our optical timescale is compared to a hydrogen maser based timescale steered to an optical lattice clock with identical uptime or a cesium fountain clock operating continuously.

hydrogen maser steered to a ^{87}Sr optical clock for 6 h/day using the same Kalman filter and noise models for the maser and fountain described in Ref. [19]. The typical performance of both timescales is assessed by computing time errors from repeated simulations [21,35], and their rms spread over a 34 day window is depicted in Fig. 3. Both exhibit a larger time error than the all-optical timescale.

Because the optical clock is run intermittently, the long-term stability of the timescale will be limited by a $1/\sqrt{\tau(s)}$ slope arising from aliased local oscillator noise akin to the Dick effect [16,19]. Determining this stability limit requires an accurate characterization of the OLO. We evaluate the stability of our OLO by analyzing the frequency noise of the residuals in Fig. 2(b). One complicating factor are the gaps in the frequency record during clock downtime. A gap-tolerant Allan variance similar to that in Ref. [36] is used to compute an estimated stability of the OLO out to multiple day averaging intervals.

The result of this analysis is plotted in Fig. 4. The OLO stability is fit to a noise model that includes the known thermal noise floor [17] and a random walk frequency noise term, resulting in an instability at long averaging times consistent with $\sigma_{\mathrm{RW}} = 1.3 \times 10^{-18}\sqrt{\tau(\mathrm{s})}$. The OLO maintains an instability below 10^{-15} out to 6×10^{5} s, more than an order of magnitude improvement over the previous characterization of this system [25]. The frequency stability of the Si-AT1 record is presented as well, and its value at averaging times past 10^{5} s agrees with the clock measurement within statistical uncertainty. At shorter averaging times, the stability is consistent with a noise model [21] accounting for instability from the microwave link, the OLO, and AT1 [37].

With an accurate noise model for the OLO in hand, we now consider the anticipated long-term stability of our timescale as a function of the optical clock duty cycle. Similar to Refs. [16,19], we simulate a lengthy local oscillator frequency record using the model presented in Fig. 4 with the drift trend from Fig. 2(a) added. This record is then steered to a simulated ^{87}Sr lattice clock for a fixed interval each day using the same Kalman filtering techniques described above. We compute an Allan deviation of the prediction error to determine the stability of the timescale. To quantify the impact of our improved local oscillator we carry out the same analysis for a similar timescale where the OLO has been substituted by a hydrogen maser. The noise model for the simulated hydrogen maser is based on the typical stability of the best performing masers in the UTC (NIST) timescale [19].

Figure 5 shows the results of our analysis. As anticipated, the long-term stability of the timescale improves with increased clock uptime and reduced local oscillator noise and is reasonably consistent with the expected instability limit from aliased local oscillator noise past 10^{6} s [21,38]. When the optical clock is run with the same duty cycle, the steered OLO significantly outperforms a steered hydrogen maser at all averaging times. Even when steering 1 h per day, our timescale is more stable than a hydrogen maser steered with a 50% duty cycle. This capability allows for a competitive timescale performance with significantly relaxed uptime requirements. Based on this analysis, we expect a stability of approximately 1.8×10^{-17} after a 34 day campaign with an average clock uptime of 6 h/day. This is in good agreement with the observed integrated time error of 48 ± 94 ps over 34 days, or $1.6 \pm 3.2 \times 10^{-17}$ in fractional units. When operating the clock 12 h per day, our all-optical timescale remains at or below the 2×10^{-16} level at all averaging times and is projected to reach a stability below 10^{-17} after only 85 days

of operation. Additional effort on automation should allow for a clock duty cycle well above 50%. Using an array of N independent silicon cavities would improve the stability by a factor of $1/\sqrt{N}$ [16].

By combining an improved local oscillator with an accurate high-uptime optical clock, we have demonstrated a novel timescale architecture with enhanced stability. Additional technical upgrades of our silicon cavity can further improve our optical timescale stability, including greater passive thermal isolation, shorter optical path lengths, and operation closer to the silicon coefficient of thermal expansion zero crossing. In addition, reducing the optical power incident on the cavity offers the capability to reduce the linear drift [24].

Future efforts will leverage existing time transfer infrastructure in Boulder, Colorado, to incorporate this optical technology into the UTC (NIST) timescale. An underground fiber network is in place to support phase-stabilized optical signal transfer from JILA to NIST with negligible excess noise [39,40]. Using a femtosecond frequency comb [41,42], our optical timescale signal will be linked to UTC.

We thank J. A. Muniz, T. R. O'Brian, A. Bauch, and J. L. Hall for their careful reading of the manuscript, and L. Sonderhouse for technical contributions. This work is supported by the National Institute of Standards and Technology, Defense Advanced Research Projects Agency, Air Force Office for Scientific Research, National Science Foundation (NSF Grant No. PHY-1734006), Physikalisch-Technische Bundesanstalt, and the Cluster of Excellence (EXC 2132 Quantum Frontiers). U.S. and T. L. acknowledge support from the quantum sensors (Q-SENSE) project supported by the European Commission's H2020 Marie Sklodowska-Curie Actions Research and Innovation Staff Exchange (MSCA RISE) under Grant Agreement No. 69115. E. O. and C. J. K. acknowledge support from the National Research Council postdoctoral fellowship.

W. R. M. and E. O. contributed equally to this work.

*william.milner@colorado.edu
†jian.yao@colorado.edu
‡Ye@jila.colorado.edu
§ericoelker@gmail.com

[1] N. Ashby, Living Rev. Relativity **6**, 1 (2003).
[2] B. M. Roberts, G. Blewitt, C. Dailey, M. Murphy, M. Pospelov, A. Rollings, J. A. Sherman, W. Williams, and A. Derevianko, Nat. Commun. **8**, 1195 (2017).
[3] P. Delva, N. Puchades, E. Schönemann, F. Dilssner, C. Courde, S. Bertone, F. Gonzalez, A. Hees, C. Le Poncin-Lafitte, F. Meynadier, R. Prieto-Cerdeira, B. Sohet, J. Ventura-Traveset, and P. Wolf, Phys. Rev. Lett. **121**, 231101 (2018).
[4] T. Takano, M. Takamoto, I. Ushijima, N. Ohmae, T. Akatsuka, A. Yamaguchi, Y. Kuroishi, H. Munekane, B. Miyahara, and H. Katori, Nat. Photonics **10**, 662 (2016).
[5] M. Lombardi, A. Novick, B. Cooke, and G. Neville-Neil, J. Res. Natl. Inst. Stand. Technol. **121**, 436 (2016).
[6] C. J. Kennedy, E. Oelker, T. Bothwell, D. Kedar, J. M. Robinson, W. R. Milner, G. E. Marti, and J. Ye (to be published).
[7] A. Bauch, S. Weyers, D. Piester, E. Staliuniene, and W. Yang, Metrologia **49**, 180 (2012).
[8] G. D. Rovera, S. Bize, B. Chupin, J. Guéna, P. Laurent, P. Rosenbusch, P. Uhrich, and M. Abgrall, Metrologia **53**, S81 (2016).
[9] B. J. Bloom, T. L. Nicholson, J. R. Williams, S. L. Campbell, M. Bishof, X. Zhang, W. Zhang, S. L. Bromley, and J. Ye, Nature (London) **506**, 71 (2014).
[10] T. L. Nicholson, S. L. Campbell, R. B. Hutson, G. E. Marti, B. J. Bloom, R. L. McNally, W. Zhang, M. D. Barrett, M. S. Safronova, G. F. Strouse, and J. Ye, Nat. Commun. **6**, 6896 (2015).
[11] W. F. McGrew, X. Zhang, R. J. Fasano, S. A. Schäffer, K. Beloy, D. Nicolodi, R. C. Brown, N. Hinkley, G. Milani, M. Schioppo, and A. D. Ludlow, Nature (London) **564**, 87 (2018).
[12] N. Huntemann, C. Sanner, B. Lipphardt, C. Tamm, and E. Peik, Phys. Rev. Lett. **116**, 063001 (2016).
[13] S. A. Brewer, J. S. Chen, A. M. Hankin, E. R. Clements, C. W. Chou, D. J. Wineland, D. B. Hume, and D. R. Leibrandt, Phys. Rev. Lett. **123**, 033201 (2019).
[14] H. Hachisu, F. Nakagawa, Y. Hanado, and T. Ido, Sci. Rep. **8**, 4243 (2018).
[15] C. Grebing, A. Al-Masoudi, S. Dörscher, S. Häfner, V. Gerginov, S. Weyers, B. Lipphardt, F. Riehle, U. Sterr, and C. Lisdat, Optica **3**, 563 (2016).
[16] J. Yao, J. A. Sherman, T. Fortier, H. Leopardi, T. Parker, W. McGrew, X. Zhang, D. Nicolodi, R. Fasano, S. Schäffer *et al.*, arXiv:1902.06858.
[17] E. Oelker, R. B. Hutson, C. J. Kennedy, L. Sonderhouse, T. Bothwell, A. Goban, D. Kedar, C. Sanner, J. M. Robinson, G. E. Marti *et al.*, Nat. Photonics **13**, 714 (2019).
[18] M. Schioppo, R. C. Brown, W. F. McGrew, N. Hinkley, R. J. Fasano, K. Beloy, T. Yoon, G. Milani, D. Nicolodi, J. Sherman *et al.*, Nat. Photonics **11**, 48 (2017).
[19] J. Yao, T. E. Parker, N. Ashby, and J. Levine, IEEE Trans. Ultrason. Ferroelectr. Freq. Control **65**, 127 (2018).
[20] T. Bothwell, D. Kedar, E. Oelker, J. M. Robinson, S. L. Bromley, W. L. Tew, J. Ye, and C. J. Kennedy, Metrologia **56**, 065004 (2019).
[21] See Supplemental Material at http://link.aps.org/supplemental/10.1103/PhysRevLett.123.173201 for a description of Kalman filter techniques and other technical experimental details.
[22] T. Kessler, C. Hagemann, C. Grebing, T. Legero, U. Sterr, F. Riehle, M. J. Martin, L. Chen, and J. Ye, Nat. Photonics **6**, 687 (2012).
[23] W. Zhang, J. M. Robinson, L. Sonderhouse, E. Oelker, C. Benko, J. L. Hall, T. Legero, D. G. Matei, F. Riehle, U. Sterr *et al.*, Phys. Rev. Lett. **119**, 243601 (2017).
[24] J. M. Robinson, E. Oelker, W. R. Milner, W. Zhang, T. Legero, D. G. Matei, F. Riehle, U. Sterr, and J. Ye, Optica **6**, 240 (2019).

[25] D. G. Matei, T. Legero, S. Häfner, C. Grebing, R. Weyrich, W. Zhang, L. Sonderhouse, J. M. Robinson, J. Ye, F. Riehle, and U. Sterr, Phys. Rev. Lett. **118**, 263202 (2017).
[26] C. Hagemann, C. Grebing, C. Lisdat, S. Falke, T. Legero, U. Sterr, F. Riehle, M. J. Martin, and J. Ye, Opt. Lett. **39**, 5102 (2014).
[27] P. Kwee, C. Bogan, K. Danzmann, M. Frede, H. Kim, P. King, J. Pöld, O. Puncken, R. L. Savage, F. Seifert, P. Wessels, L. Winkelmann, and B. Willke, Opt. Express **20**, 10617 (2012).
[28] E. Oelker, L. Barsotti, S. Dwyer, D. Sigg, and N. Mavalvala, Opt. Express **22**, 21106 (2014).
[29] D. J. Ottaway, P. Fritschel, and S. J. Waldman, Opt. Express **20**, 8329 (2012).
[30] M. Bishof, X. Zhang, M. J. Martin, and J. Ye, Phys. Rev. Lett. **111**, 093604 (2013).
[31] G. K. Campbell, A. D. Ludlow, S. Blatt, J. W. Thomsen, M. J. Martin, M. H. de Miranda, T. Zelevinsky, M. M. Boyd, J. Ye, S. A. Diddams *et al.*, Metrologia **45**, 539 (2008).
[32] J. Levine, Rev. Sci. Instrum. **83**, 020901 (2012).
[33] J. Yao, T. E. Parker, and J. Levine, Meas. Sci. Technol. **28**, 115004 (2017).
[34] A. Gelb, *Applied Optimal Estimation* (MIT Press, Cambridge, MA, 1974).
[35] S. Weyers, V. Gerginov, M. Kazda, J. Rahm, B. Lipphardt, G. Dobrev, and K. Gibble, Metrologia **55**, 789 (2018).
[36] I. Sesia and P. Tavella, Metrologia **45**, S134 (2008).
[37] W. F. McGrew, X. Zhang, H. Leopardi, R. J. Fasano, D. Nicolodi, K. Beloy, J. Yao, J. A. Sherman, S. A. Schäffer, J. Savory, R. C. Brown, S. Römisch, C. W. Oates, T. E. Parker, T. M. Fortier, and A. D. Ludlow, Optica **6**, 448 (2019).
[38] G. J. Dick, in *Proceedings of the 19th Annual Precise Time and Time Interval Meeting, Redondo Beach, CA, 1987* (U.S. Naval Observatory, 1988), pp. 133–147.
[39] S. M. Foreman, K. W. Holman, D. D. Hudson, D. J. Jones, and J. Ye, Rev. Sci. Instrum. **78**, 021101 (2007).
[40] S. M. Foreman, A. D. Ludlow, M. H. G. de Miranda, J. E. Stalnaker, S. A. Diddams, and J. Ye, Phys. Rev. Lett. **99**, 153601 (2007).
[41] H. Leopardi, J. Davila-Rodriguez, F. Quinlan, J. Olson, J. A. Sherman, S. A. Diddams, and T. M. Fortier, Optica **4**, 879 (2017).
[42] T. M. Fortier, A. Bartels, and S. A. Diddams, Opt. Lett. **31**, 1011 (2006).